Influence of Costal Cartilage Geometry on Rib Strain in THUMS under Frontal Hub Impact

Takuma Miyazaki, Yoshiki Takahira, Hiroaki Imai, Mitsuhiro Hamada, Yuji Nakane

I. INTRODUCTION

Thoracic injuries account for a significant proportion of AIS2+ injuries in vehicle crashes [1]. To enhance injury prediction, human body models (HBMs) are increasingly being used alongside anthropomorphic test devices (ATDs). The introduction of a strain-based rib fracture risk assessment into consumer vehicle safety ratings is anticipated. However, the Total Human Model for Safety (THUMS) has been reported to underestimate rib fracture risk, notably NFR3+ risk under frontal chest hub impactor conditions for elderly occupants, attributed to costal cartilage geometry [2].

This study aims to (1) evaluate whether the costal cartilage geometry in THUMS is wider than average male anthropometry, and (2) investigate whether narrowing the costal cartilage improves predicted rib fracture risk under frontal hub impact conditions.

II. METHODS

Generation of modified model

First, the costal cartilage geometry of the original THUMS AM50 v7.1 model was compared with literature data [3] by evaluating the distance between the rib end (ribs 1–7) and the corresponding sternal attachment, and comparing it with values from the regression model in [3] for a 40-year-old, 77.3 kg male. Based on the comparison, a modified THUMS was created. In the modified model, a subset of the shell and solid elements originally representing the costal cartilage of ribs 2–7 in the base model was reallocated to the rib, while the remaining rib elements were kept unchanged; the added shell elements were assigned a constant thickness.

Investigation under chest hub impactor condition

For comparison, the VIVA+ 50M v2.0.2 model [4] was also included. All models were subjected to a frontal hub impact simulation (impactor mass: 23.4 kg, velocity: 6.7 m/s) [5]), using the HBM4VT validation set-up [6]. The posture of THUMS was further adjusted from the HBM4VT configuration by rotating the model about the y-axis to align the impactor trajectory perpendicular to the sternum, with the aim of improving the fidelity to the experimental set-up. The NFR3+ risk (probability of three or more rib fractures) were derived from the maximum principal strain (MPS) values using the risk curve generated from experimental data [7].

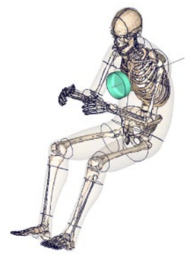

Fig. 1. Chest Impactor.

Single-rib bending simulation

To isolate the influence of rib geometry from whole-thorax loading, a single-rib bending simulation was performed. A representative mid-level rib (rib 4) was extracted from each model and subjected to a dynamic bending condition using prescribed displacement control, with one rib end translationally constrained and the opposite end displaced; rotational degrees of freedom were permitted at both ends.

The same loading configuration was applied to THUMS, VIVA+, and a hybrid model in which the VIVA+ rib material card was assigned to the THUMS rib geometry. Force–deflection responses were evaluated and compared against published post-mortem human subject (PMHS) corridors [8].

III. INITIAL FINDINGS

The costal cartilage in THUMS was found to be wider than the average male anthropometry (Fig. 2 and Fig. 3). The modified THUMS model showed increased rib strain compared to the original, but still lower than VIVA+. The NFR3+ risk increased by 7.6 percentage points but remained lower than that of VIVA+ (Fig. 4). In PMHS experiments, three or more rib fractures were observed only in elderly subjects aged 72 and 80 years, but not in younger subjects [5].

T. Miyazaki (e-mail: takuma.miyazaki@toyota-europe.com) is an engineer, Y. Takahira is an assistant manager, H. Imai is a group manager, M. Hamada is a general manager and Y. Nakane is a project general manager, all in Vehicle Engineering Development Division at Toyota Motor Corporation, Japan.

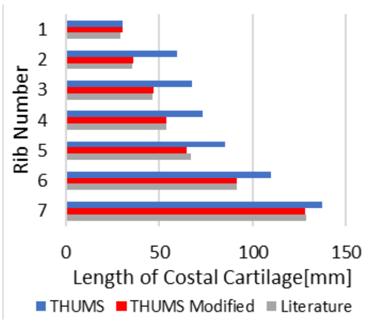

Fig. 2. Length of costal cartilage.

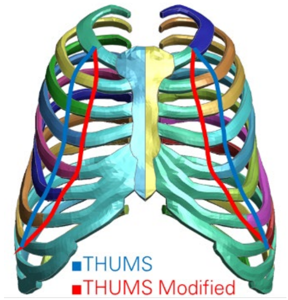

Fig. 3. Modification overview.

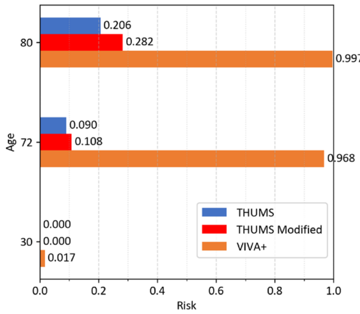

Fig. 4. Predicted NFR3+ risk.

IV. DISCUSSION

The results indicate that modifying the costal cartilage geometry alone does not fully resolve the underestimation of rib fracture risk in THUMS. Force-stroke (F-S) analysis (Fig. 5) showed that THUMS exhibited higher impactor force during the second peak (rib deformation phase) compared to VIVA+, although both remained within PMHS corridors [9].

To compare the load transmitted to the ribs, cross-sectional rib forces were evaluated at the anterior rib ends using identical x-coordinates (Fig. 6). The cross-sectional forces were generally comparable between THUMS and VIVA+, except for the interval between 10 ms and 20 ms. These results indicate that, despite differences in impactor force, the input load transmitted to the ribs was largely similar. Nevertheless, the resulting rib deformations differed between the models.

Single-rib bending simulations (Fig. 7) showed that THUMS ribs are stiffer than those in VIVA+, although both remained within PMHS corridors [9]. Considering the results described above, when comparable input loads were applied to the rib, THUMS exhibited smaller rib deformation (strain) than VIVA+. Additional simulations using the VIVA+ material card transplanted into THUMS confirmed that the stiffness difference arises from anthropometric differences in rib shape and cross-sectional geometry, with cortical shell thickness also contributing, ranging from 0.25 to 1.91 mm in THUMS and 0.18 to 1.83 mm in VIVA+. Previous work has also reported that the rib cross-sectional area of average male HBMs, including THUMS, is larger than that of the average male population, with deviations exceeding one standard deviation depending on rib level and location [10].

These findings suggest that addressing the underestimation of rib strain in THUMS requires analysis and countermeasures beyond costal cartilage geometry alone. Multiple contributing factors must be considered. Further investigation is needed to better understand the factors contributing to the differences in rib strain observed across different HBMs.

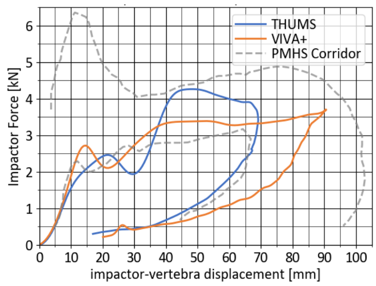

Fig. 5. Impactor Force–stroke plot.

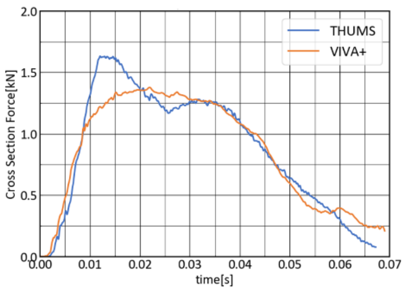

Fig. 6. Cross-sectional force.

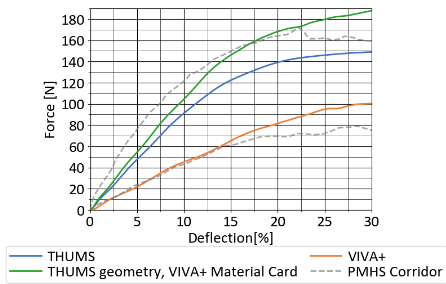

Fig. 7. Single-rib bending Force–stroke plot.

V. REFERENCES

[1] Ostling, M., *et al.*, *IRCOBI*, 2024.
[2] Kannan, V., *et al.*, *IRCOBI*, 2025.
[3] Gayzik, F., *et al.*, *J Biomech*, 2008.
[4] https://vivaplus.readthedocs.io/en/latest/.
[5] Kroell, C. K., *et al.*, *Stapp*, 1971.
[6] https://openvt.eu/EuroNCAP/hbm4vt-validation-catalogue/ls-dyna/kroell_1971.
[7] Larsson, K., *et al.*, *Front Bioeng Biotechnol*, 2021.
[8] Kang, Y., *et al.*, *Ann Biomed Eng*, 2020.
[9] Lebarbe, M., Petit, P., *IRCOBI*, 2012.
[10] Holcombe, S., et al., Front Bioeng Biotechnol, 2023.

AI Disclosure: An AI tool (Microsoft Copilot) was used in a supporting role during manuscript preparation. Authors maintained full oversight and responsibility for all content.